MECHANISM OF SHRINKAGE CRACKING OF SOIL-CEMENT BASES

K. P. George, Department of Civil Engineering, University of Mississippi

In recognition of the importance of shrinkage-induced stresses in the overall problem, various theories to predict the stresses are reviewed and a few results presented. A theory of cracking is advanced stating that the microcracks are initiated in the vicinity of pre-existing flaws; with increasing shrinkage stress the microcracks coalesce to form macrocracks. The crack propagation (deepening or lengthening) is shown to be governed by the crack extension force. The crack spacing in pavements is shown to be a function of shrinkage stresses, strength of the material, and stress relief surrounding the individual cracks. A mechanism for longitudinal cracking is proposed, based on the principle that cracks first appear in the subgrade and are afterwards reflected through the soil-cement base.

•SHRINKAGE cracking is one of the unsatisfactory aspects of the overall behavior of soil-cement bases. At the time of occurrence it has relatively little effect on the riding quality of highway pavement. Its implications or "secondary deterioration" effects, however, such as reflection and the resultant weakening of the subgrade, can be highly detrimental to the performance and useful life of the pavement structure.

The tacit assumption in predicting cracking in soil-cement, concrete, or asphalt pavement is that a layer will crack when the induced stresses, either externally applied or internally developed, exceed the tensile strength of the material (5, 6, 8). Externally applied stresses may be due to traffic or to "drag" from subgrade cracking, whereas the internally developed stresses are thought to be associated primarily with drying and/or temperature changes. The important factors contributing to cracking, therefore, are (a) stresses induced by traffic load, by diurnal and seasonal thermal variation, and by drying shrinkage, and (b) shrinkage cracking of the subgrade and subsequent reflection cracking.

Although the mechanisms of shrinkage cracking are emphasized in this paper, with slight modification the analysis can well be adapted for thermal cracking. The present analysis is founded on the premise that, under tension, small flaws start to grow and coalesce to form microcracks and, eventually, macrocracks. By investigating the stresses and displacements in the subgrade by a finite-element analysis, we also investigate the mechanics of reflection cracking.

In the present study we have explored the phenomenon of shrinkage-induced cracking (fracture) of soil-cement bases, with special reference to crack initiation and propagation. An adequate understanding of the pertinent mechanisms involved is essential to the eventual development of control or predictive techniques relating to fracture susceptibility. Accordingly, the following aspects are discussed in this paper:

1. Estimation of internally developed shrinkage-induced stresses;
2. Flaws and microcracks in cement base and their role in initiating cracks;
3. Initiation and propagation of macrocracks;
4. Spacing and configuration of cracked panels with special reference to the random nature of cracked panels; and
5. Reflection cracking with emphasis on longitudinal cracks.

Publication of this paper sponsored by Committee on Soil-Portland Cement Stabilization.

A systematic study of shrinkage cracking phenomena in soil-cement bases must necessarily consider the calculation of shrinkage-induced stresses.

In the case of uniform shrinkage, the stress calculation is simplified by considering the pavement base as an elastic, infinitely long beam of finite width. The unit tensile stress in the longitudinal direction, σ_{xx}, is given by

$$\sigma_{xx}(S) = ES$$

where E = Young's modulus and S = free, unrestrained shrinkage.

As for the linear shrinkage, we know that if a pavement slab is subjected to a uniform temperature and/or shrinkage gradient its surface will tend to warp. Westergaard (15) solved the problem of a slab of finite width and infinite length supported on a Winkler foundation. Harr and Leonards (4) solved a similar problem for a circular slab wherein they considered the possibility that warping may result in only partial support of the slab by the foundation. In the event the shrinkage is linear but is not symmetrical with respect to the central plane, the stresses in a free slab can be computed if the thickness of the slab is known.

For the nonuniform shrinkage gradient, Thomlinson (13) as early as 1940 modified Westergaard's approach by assuming a single harmonic temperature variation at the top surface of the slab. Applying the laws of heat flow, Thomlinson arrived at a curved temperature gradient through the depth of the slab which enabled him to solve for stresses and deflections. Reddy et al. (10) presented a theory that accounts for warping produced by nonlinear temperature and moisture variations of sufficient magnitude to result in a partially supported slab.

Monismith et al. (8) utilized the equations developed by Humphreys and Martin (7) and presented stress field equations in an asphalt slab as a function of depth and time.

Pretorius (9) studied the shrinkage stresses in a cement-treated base bounded by an asphalt surface and subgrade beneath. The viscoelastic analyses indicated uniform shrinkage to be of minor importance where the magnitude of stresses varied according to the restraint offered to soil-cement shrinkage by the other layers in the pavement. Figure 1 shows the stress results in a pavement slab subjected to an initial differential humidity distribution of 85 to 90 percent that desiccates to a uniform 85 percent condition within 30 days. Also shown is the stress variation for the uniform shrinkage at 85 percent. The results appear realistic in spite of the fact that an arbitrary humidity distribution was chosen for calculations.

Sanan and George (11) studied shrinkage stresses in soil-cement pavement slabs (long strip) supported on a subgrade (Winkler foundation) and subjected to one-dimensional drying from the top face of the slab. To analyze shrinkage strain distribution, it is assumed that the moisture movement obeys the diffusion equation and shrinkage is proportional to the moisture loss. Figure 2 shows that, theoretically, regardless of the restraint condition, shrinkage stress is highly localized on the exposed surface and decreases sharply with depth. This solution is modified by considering that moisture movement obeys capillary flow theory (3).

We have indicated in this brief summary of shrinkage stress in a drying soil-cement slab that the stress can be expressed as a function of drying time and depth of slab. A theory of cracking is advanced that the microcracks are initiated in the vicinity of preexisting flaws; with increasing shrinkage stress, the microcracks coalesce to form macrocracks. This paper emphasizes the impact of inadvertent flaws on the fracture process.

The significance of flaw distribution was recognized first by Weibull (14), who assumed that the local strength of the material obeys a power law. That the strength of the material decreases with size and increases with the homogeneity of the material is expressed in a single relation for "risk of rupture",

$$B = n(\sigma)dv$$

where dv = elemental volume and

Figure 1. Time variation of shrinkage stress, viscoelastic analysis (9).

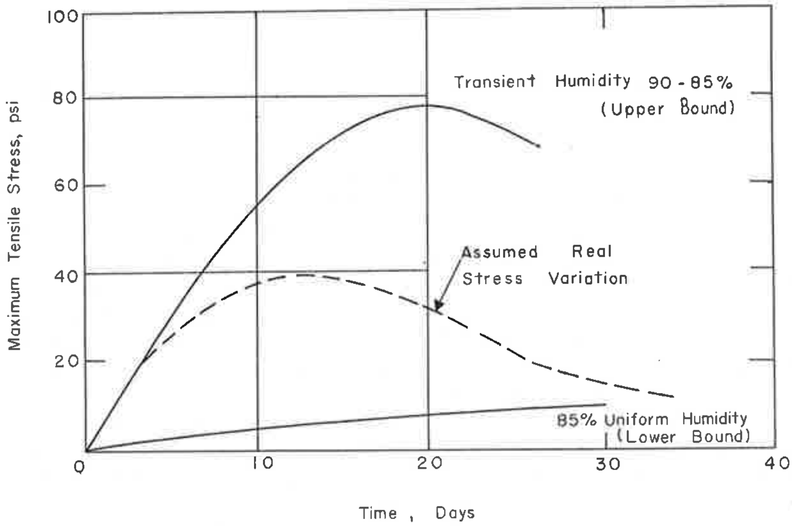

Figure 2. Shrinkage stress versus drying time.

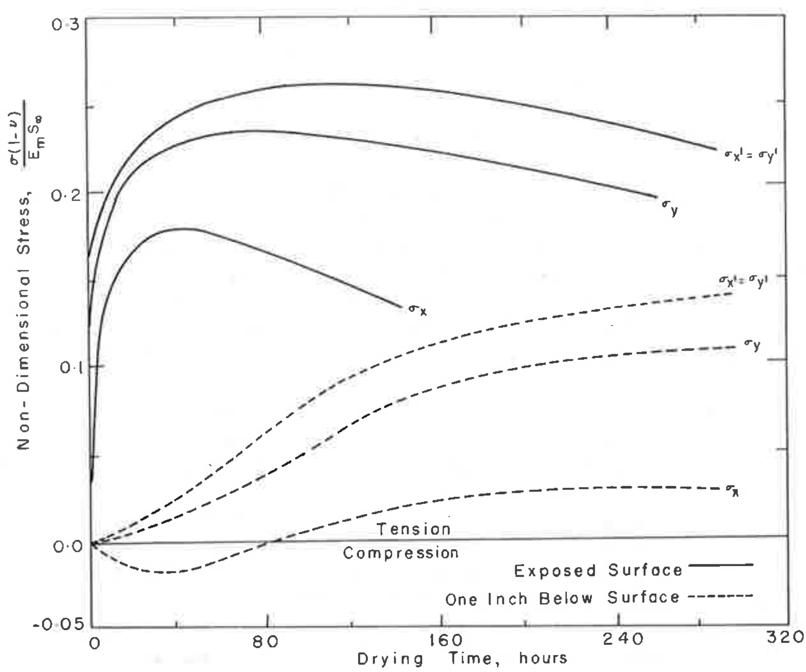

$$n(\sigma) = \left(\frac{\sigma}{\sigma_0}\right)^m$$

in which σ = the desired strength and m, σ_0 = constants of the material. The factor m is a characteristic of the degree of homogeneity of the material and is larger the higher the homogeneity.

A soil-cement base is built by compacting a mixture of soil and cement at optimum moisture. Compaction is usually accomplished by sheepsfoot rollers followed by pneumatic-tired or steel-wheeled tandem rollers. In order to illustrate how heavy rollers induce microcracks, we consider a typical 8-ton roller (4 ft wide, 4 ft in diameter) compacting a 10-in. soil-cement base that has acquired a shear strength of θ = 20 deg and c = 50 psf. Assuming a coefficient of rolling resistance of 3 in., a triangular stress distribution (Fig. 3a) is assumed immediately beneath the roller. Limiting equilibrium calculations (12) reveal that unless a distributed load (Fig. 3b) is applied immediately behind the roller a bearing capacity failure is likely to occur. During rolling, therefore, a slip plane, approximately perpendicular to the road surface and transverse to the direction of rolling, is induced in the base. Although these slip planes would be "healed" during curing, they present weak planes in the slab. Since all cracks can be visulaized as initiating at zones of weakness or flaws, these shear planes serve as the primary seat for further cracking.

This simplified analysis further reveals that rollers similar to pneumatic rubber-tired rollers, in which the tires are arranged in two or three rows, create fewer slip planes than steel-wheeled rollers, in which the entire load is transmitted through one single axle. It may also be conjectured that a vibratory roller would produce fewer cracks than static rollers.

It takes energy to lengthen a crack, first, to overcome the forces of cohesion to produce new surfaces and, second, in a brittle plastic medium, to do the work of plastic deformation in the region of elevated stress near the crack tip. Thus a crack will lengthen if, and only if, by so doing it releases at least as much strain energy as it consumes near the crack tip.

Figure 4 shows the shrinkage stresses as a function of depth, calculated according to continuum theory (9). Comparing the stress distribution and the G-force with respect to depth, it is noted that, although the stress before cracking passes from tension to compression at approximately 3 in. depth, this horizon has no particular significance insofar as propagation of the crack is concerned. After entering the compressional field, a tension crack continues to release deformation energy. The crack in the example probably would not be arrested until it reached a depth of 4 in., where G declines sharply.

The schematic representations in Figure 5 show crack initiation and propagation in a finite series of steps due to drying shrinkage alone. It can be shown that, as the shrinkage advances into the slab, similar to that shown in Figure 5b, the base, being restrained by the subgrade, will experience somewhat uniform tensile stress (1).

The spacing of tension cracks is probably determined by three quite independent factors: (a) shrinkage and/or thermal stresses in the pavement slab, (b) variation of material strength from place to place (flaw distribution), and (c) width of zone of stress relief surrounding the individual cracks. The stress distribution near a single isolated transverse crack in a long infinitely wide slab is shown in Figure 6, which clearly illustrates that each crack has associated with it a zone of stress relief (15). Beyond about 4 ft in this example, the surface stresses are not affected by the cracks in this region, and therefore other cracks would be expected to occur.

As the surficial tensile stresses build up, the strength will be exceeded first at the largest flaws. Cracks spreading these flaws will trace sinuous courses, generally following zones of weakness and following the direction perpendicular to the maximum principal stress. These transverse cracks will be widely spaced because large flaws are rare, and spacing will be irregular because such flaws are distributed randomly. After the crack has formed, however, the isotropy of the stress field is destroyed in a band surrounding the crack, its zone of stress relief, although at large distances a small stress relief would eventually be dominated by local variations caused by flaws.

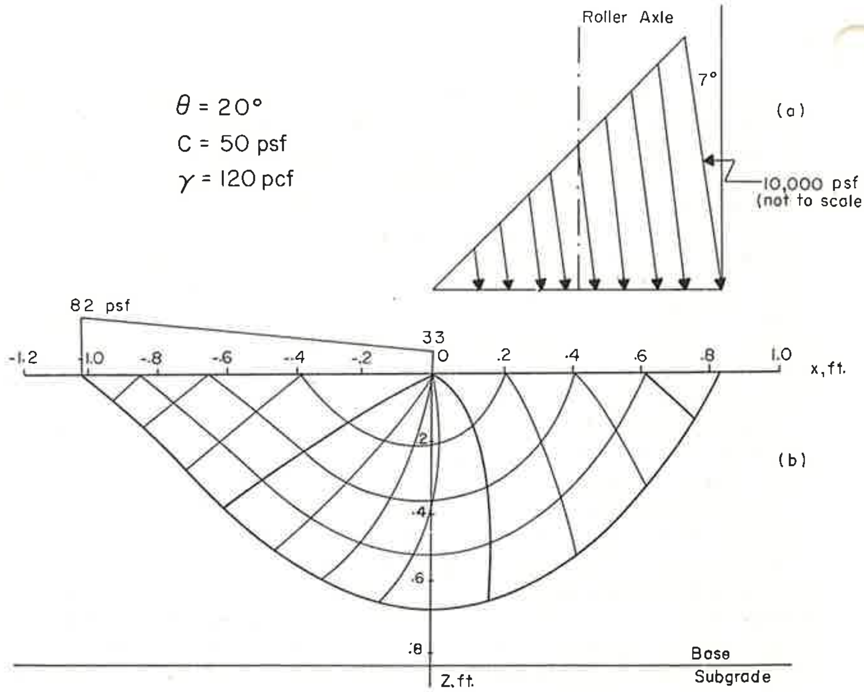

Figure 3. (a) Stress distribution under an 8-ton roller. (b) Slip lines due to stress distribution as in (a); pressure for limiting equilibrium varies from 82 to 33 psf.

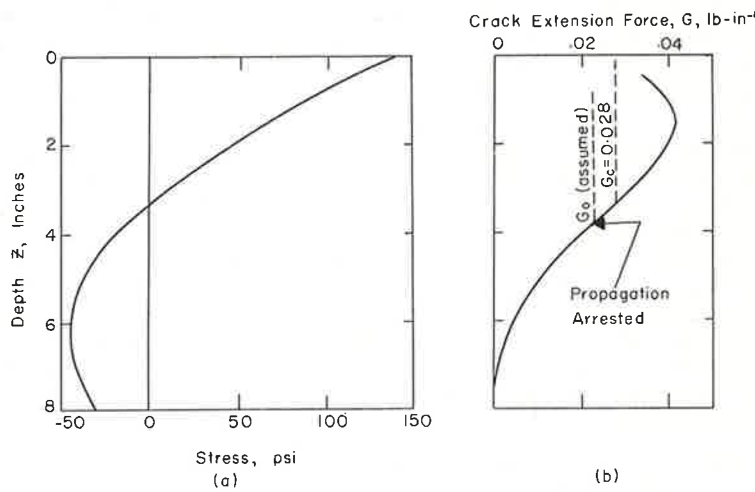

Figure 4. Shrinkage stresses as a function of depth: (a) Typical shrinkage stress distribution (9); (b) crack extension force corresponding to stress in (a).

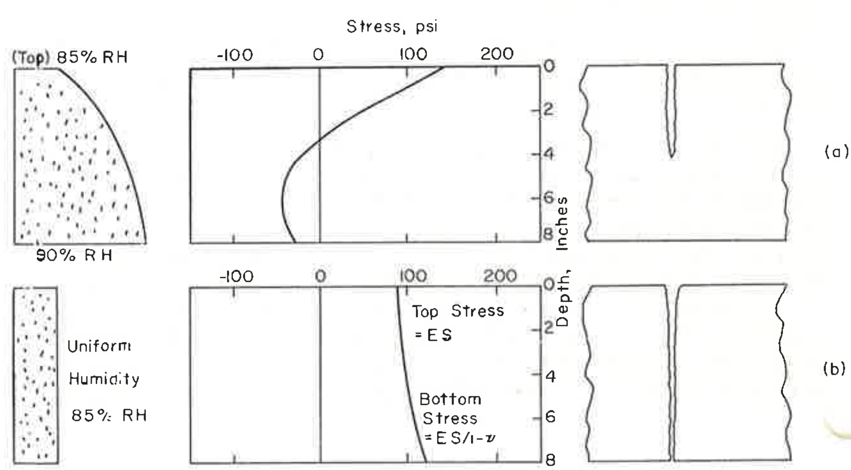

Figure 5. (a) Crack initiated due to localized surface (tension) stress; stress distribution same as in Figure 4(a). (b) Crack propagated through due to continued shrinkage.

Further cracking under increased shrinkage tension will continue to be controlled by the positions of randomly distributed flaws (Fig. 7). That is, so long as the shrinkage stress does not exceed the small sample strength, the spacing would be somewhat irregular. As the tension is further increased so that the stress exceeds the strength, every point on the surface is subject to a stress relief from at least one crack (Fig. 7c). At this stage, the series of events leading to cracks would indicate that if τ_s/τ is less than unity rather regular crack spacing can be expected; if the ratio is greater than unity, irregular spacing will tend to occur. In support of this hypothesis, the distribution of crack spacing in two cement bases, 13 percent and 7 percent respectively, is shown in Figure 8. Other factors being equal, especially the shrinkage stress, T, in the two sections, the less uniform spacing in the 13 percent base can well be attributed to the higher value of τ_s/τ.

In the discussion of crack spacing, it has been assumed that cracks are parallel. As cracking progresses, however, the traces of cracks on the pavement surface tend to form closed polygons.

Polygonal cracking is associated with successive thermal contraction, and this phenomenon is preferentially observed in materials in which the ratio of strength to stress is nearly unity. Consider a cement base that, due to drying shrinkage, exhibits a system of transverse cracks (Fig. 9). Where the crack trends north-south, the east-west tension falls to zero, while for a straight crack, the north-south tension persists at roughly three-fourths of its precracking value. Where the crack curves, the tangential component is somewhat greater on the convex side and somewhat less on the concave side. A second crack, randomly propagating across the surface, might alter its path in such a way that it tended to be perpendicular to the greatest tension and therefore would intersect the first crack at right angles. When large flaws are interconnected by distinct cracks, a few of the once-minute cracks may become large-size flaws, resulting in more surface cracks. This progressive subdivision of the surface under increasing stress could lead to a crack pattern in which orthogonal intersections predominate. Since neither the first cracks nor the later ones are oriented directionally, the pattern could be described as "random orthogonal polygons" (Fig. 10).

The spacing of transverse cracks is shown to be a function of the tensile strength of soil-cement; we have reported (2), however, that the spacing of longitudinal cracking is independent of the strength.

The effect of subgrade shrinkage is investigated by a plane strain finite-element displacement formulation. The cross section investigated, with the appropriate boundary conditions, is shown in Figure 11. The section studied is bounded by a cracked vertical face (AB in Fig. 11) on the left and the centerline (CL) on the right. Initial shrinkage strains, E_o, as shown in Figure 12, are induced in the outer shell of the subgrade. When the displacements and stresses are summarized they lead to the following observations:

1. The subgrade is stressed very highly at approximately 2 ft from the cracked edge AB (area in tension is shaded).
2. The displacement pattern in Figure 12 shows a zero displacement zone 40 in. from the cracked edge.
3. Close to the centerline, the tensile stress in the cement base is close to its strength level, a condition that could result in a longitudinal crack in the vicinity of the construction joint.

The stress distribution in the subgrade, however, suggests cracking of the subgrade and propagation of these cracks through the soil-cement base. In order to formalize the theory of "reflection cracking", we consider a section (Fig. 13) bounded at one end by the centerline, CL (or any other axis that is practically not displaced horizontally and located somewhere beyond the front of moisture changes in the subgrade), and at the other end by axis AB, representing a crack or a free end.

As the shrinkage front moves toward the centerline (for example, through successive points A_1, A_2, A_3), the stress in the shrinking subgrade increases; and when the force equals the strength level, cracking begins. We assume that the continuity between the subgrade and the base still exists, an assumption that is nearly true except for the

Figure 6. Stress relief due to a free edge at y = 0. Shrinkage strain S is linearly distributed. The slab has an edge along the axis of x and extends indefinitely in positive and negative x and positive y (15); E = 305,000 psi, k = 225 psi/in., ν = 0.25, h = 8 in.

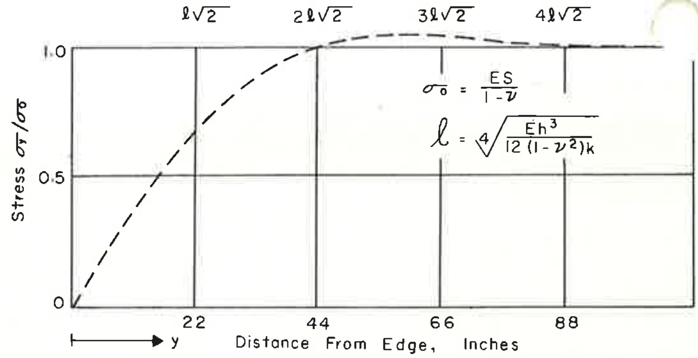

Figure 7. Variation of surface stress during the evolution of shrinkage cracks: τ = shrinkage stress that would exist on an unfractured surface; τ_s = the small sample strength. (a) Initial crack position controlled by that of largest flaw; (b) crack positions controlled by those of flaws weaker than τ_s; hence, (c) crack positions controlled by stress relief from pre-existing cracks.

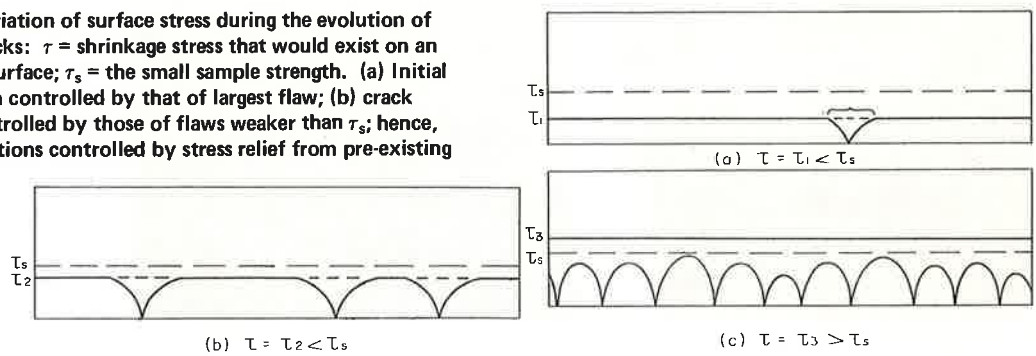

Figure 8. Spacing of transverse cracks in the experimental soil-cement bases of 13 and 7 percent cement (2).

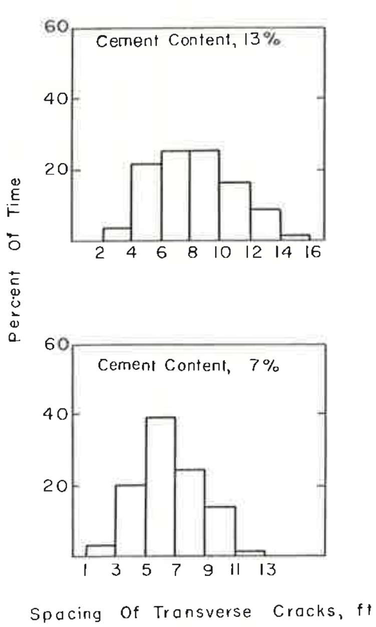

Figure 9. Transverse cracking.

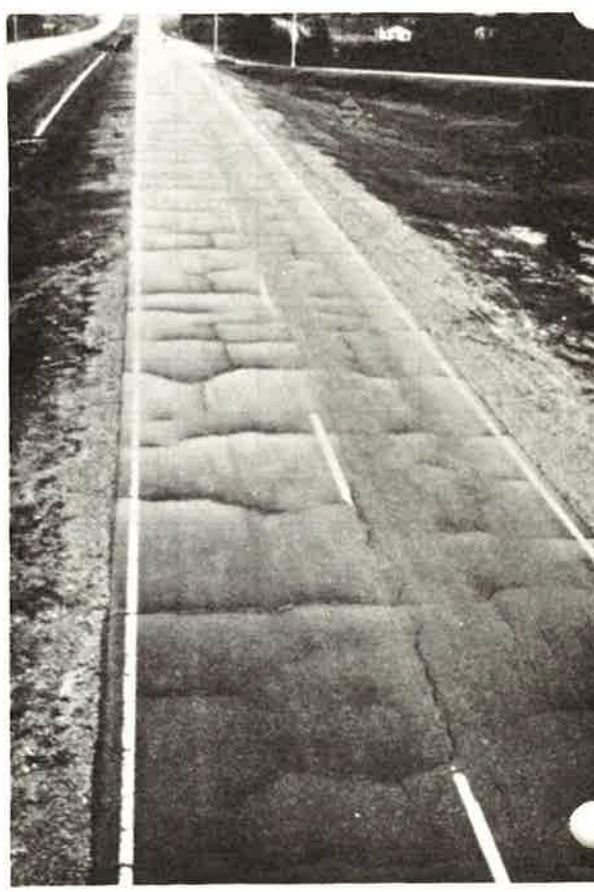

Figure 10. Polygonal cracking.

Figure 11. Cross section investigated: Top 2 rows (italic numerals) show soil-cement stress, σ_x (psi); bottom rows show shrinkage strain in subgrade, $\epsilon_0 \times 10^{-4}$.

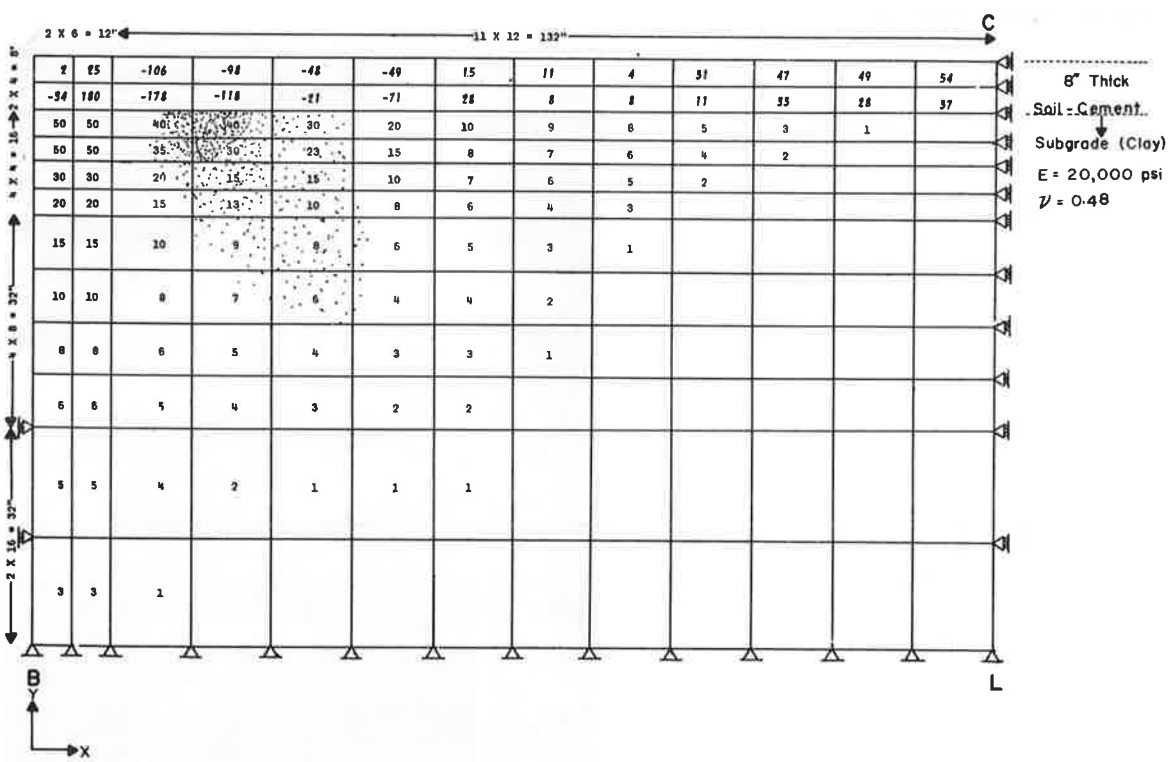

Figure 12. Cross section investigated: Displacement pattern.

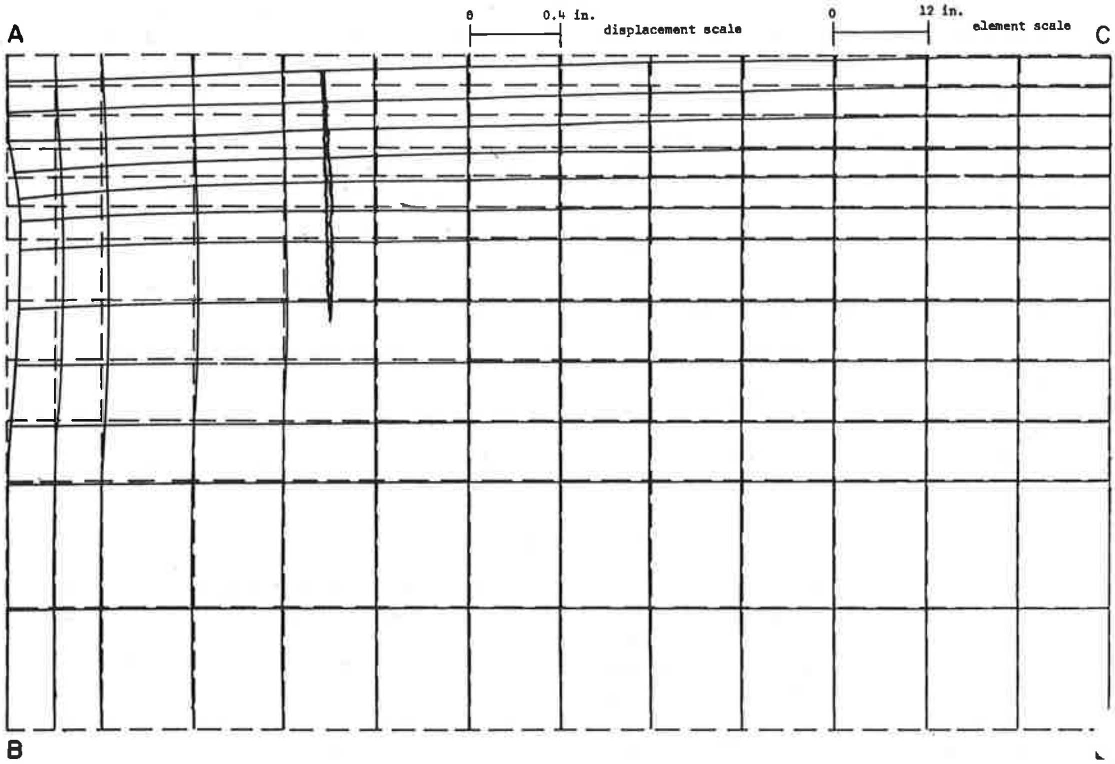

Figure 13. Proposed cracking mechanism: (a) Shear stress at base-subgrade interface; (b) crack developed in the subgrade, subsequently reflected through base.

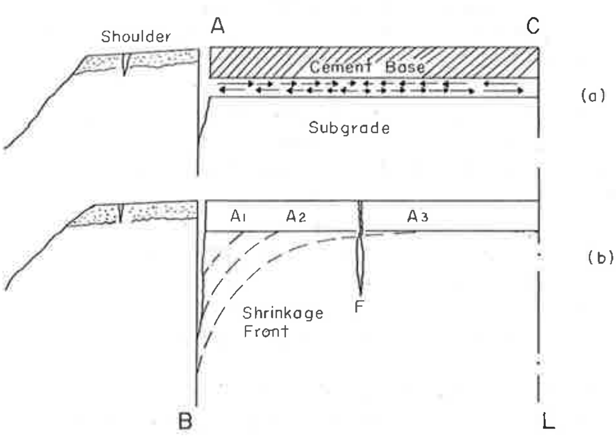

immediate vicinity of the subgrade crack. With further drying of the subgrade, due to the drag force, the crack at F propagates through the soil-cement base and successively through other layers to the surface, after which another new cracking cycle begins. The crack front thus advances toward the centerline, with A_3F assuming the role of AB, and CL (or any other intermediate section) assuming the role of zero displacement section.

In summary, the underlying principle of the proposed mechanism is that cracks are initiated in the subgrade and subsequently are reflected through the base. The subgrade had previously cracked under the combined action of shrinkage by drying and the resistance to shrinkage due to the soil-cement base on the one hand and to the deep, constant-moisture layers of the clay on the other.

This paper attempts to rationalize the mechanics of shrinkage cracking in soil-cement bases. The findings may be summarized as follows:

1. Stress due to shrinkage and/or thermal variations can be calculated to predict cracking;
2. Under stress small flaws start to grow and coalesce to form microcracks and macrocracks;
3. A mechanism for crack deepening and crack propagation is proposed; and
4. Longitudinal cracks are shown to be primarily reflection cracks.

REFERENCES

1. Durelli, A. J., and Parks, C. J. R. Stresses in Square Slabs, With Different Edge Geometries, When Bonded on One Face to a Rigid Plate and Shrunk. Experimental Mechanics, Vol. 7, 1967, pp. 481-484.
2. George, K. P. Base Course Mix Design Criteria for Cement Treated Loess. Ph.D. thesis, Iowa State University, Ames, 1963.
3. George, K. P. Shrinkage Cracking of Soil-Cement Base: Theoretical and Model Studies. Highway Research Record 351, 1971, pp. 115-133.
4. Harr, M. E., and Leonards, G. A. Warping Stresses and Deflections in Concrete Pavements. HRB Proc., Vol. 38, 1959, pp. 286-321.
5. Haas, R. C., and Topper, T. H. Thermal Fracture Phenomena in Bituminous Surfaces. HRB Spec. Rept. 101, 1969, pp. 136-153.
6. Hajek, J. J., and Haas, R. C. G. Predicting Low-Temperature Cracking Frequency of Asphalt Concrete Pavements. Highway Research Record 407, 1972, pp. 39-54.
7. Humphreys, J. S., and Martin, C. J. Determination of Transient Thermal Stresses in a Slab With Temperature-Dependent Viscoelastic Properties. Trans. Society of Rheology, Vol. 7, 1963.
8. Monismith, C. L., Secor, G. A., and Secor, K. E. Temperature Induced Stresses and Deformations in Asphalt Concrete. Proc. AAPT, Vol. 34, 1965.
9. Pretorius, C. P. Design Considerations for Pavements Containing Soil Cement Bases. Ph.D. thesis, Univ. of California, Berkeley, April 1970.
10. Reddy, A. S., Leonards, G. A., and Harr, M. E. Warping Stresses and Deflections in Concrete Pavements: Part III. Highway Research Record 44, 1963, pp. 1-24.
11. Sanan, B. K., and George, K. P. Viscoelastic Shrinkage Stress in Soil-Cement Base. Jour. Soil Mech. and Found. Div., Proc. ASCE, Vol. 98, Dec. 1972.
12. Sokolovsky, V. V. Statics of Soil Media. Butterworth's Scientific Publications, London, 1960.
13. Thomlinson, J. Temperature Variations and Consequent Stresses Produced by Daily and Seasonal Temperature Cycles in Concrete Slabs. Conc. and Const. Eng., 1940.
14. Weibull, A. Statistical Theory of the Strength of Materials. Jour. Appl. Mechanics, Vol. 18, 1946.
15. Westergaard, H. M. Analysis of Stresses in Concrete Pavements Due to Variations of Temperature. HRB Proc., Vol. 6, 1926, pp. 201-215.